Thermal Conductivity and Dynamic Mechanical Property of Glycidyl Methacrylate-Grafted Multiwalled Carbon Nanotube/Epoxy Composites

Chih-Chun Teng,[1] Chen-Chi M. Ma,[1] Shin-Yi Yang,[1] Kuo-Chan Chiou,[2] Tzong-Ming Lee,[2] Chin-Lung Chiang[3]

[1]*Department of Chemical Engineering, National Tsing Hua University, Hsin-Chu 30043, Taiwan*
[2]*Material and Chemical Research Laboratories, Industrial Technology Research Institute, Hsin-Chu 31040, Taiwan*
[3]*Department of Safety, Health and Environmental engineering, Hung Kuang University, Taichung 443, Taiwan*

Received 19 October 2010; accepted 18 March 2011
DOI 10.1002/app.34580
Published online 9 August 2011 in Wiley Online Library (wileyonlinelibrary.com).

ABSTRACT: The well dispersed multiwalled carbon nanotube (MWCNT)/epoxy composites were prepared by functionalization of the MWCNT surfaces with glycidyl methacrylate (GMA). The morphology and thermal properties of the epoxy nanocomposites were investigated and compared with the surface characteristics of MWCNTs. GMA-grafted MWCNTs improved the dispersion and interfacial adhesion in epoxy resin, and enhanced the network structure. The storage modulus of 3 phr GMA-MWCNTs/epoxy composites at 50°C increased from 0.32 GPa to 2.87 GPa (enhanced by 799%) and the increased tanδ from 50.5°C to 61.7°C (increased by 11.2°C) comparing with neat epoxy resin, respectively. Furthermore, the thermal conductivity of 3 phr GMA-MWCNTs/epoxy composite is increased by 183%, from 0.2042 W/mK (neat epoxy) to 0.5781 W/mK. © 2011 Wiley Periodicals, Inc. J Appl Polym Sci 123: 888–896, 2012

Key words: nanocomposites; thermal properties; carbon nanotubes

INTRODUCTION

Carbon nanotubes (CNTs) possess unique structural, mechanical, thermal, and electrical properties. As a result, they have extensive applications in various fields.[1] Due to the fact that most polymers possess a low thermal conductivity, the introduction of high thermal conductivity of CNTs is an effective method to enhance the thermal transport of polymer composites. High thermal conductive composites could be used for printed circuit boards and electronic devices. However, CNTs generally form agglomerated stabilized bundles due to the Van der Waals force. They are difficult to disperse in conventional solvents and polymer matrix, and are extremely resistant to wetting.[2] Moreover, the weak interfacial bonding between CNTs and polymer matrices may limit the load transfer of stress. Previous studies have investigated the dispersion and reinforcement of CNTs in a polymer matrix, including noncovalent and covalent functionalization.[3–5] Several studies reported the functionalization of CNTs and grafting with polymer chains via free radical polymerization.[6–11] CNTs can well disperse in the polymer matrix via free radical polymerization, such as poly(methyl methacrylate), polystyrene and etc,. Results indicate that the free radical initiators can activate CNTs to open their π-bonds, and that CNTs participate in the additional polymerization of the monomer. Therefore, the polymer chains will be grafted onto the surface of the CNTs, forming a strong interfacial bonding between CNTs and polymer matrix.

Major modifications approach to enhance the interface adhesion between epoxy and CNTs are based on amino-functionalized CNTs.[12,13] Amino-functionalized CNTs may act as a curing agent and react with the epoxy matrix during the curing process and build a covalent linkage. On the basis of these concepts, Glycidyl methacrylate (GMA) was used and grafted on the MWCNT sidewalls via free radical polymerization. These reactive MWCNTs possess oxirane rings that can improve their affinity to the epoxy matrix and react with the amino group of the curing agent to form a highly cross-linked structure with covalent bonds between MWCNTs and epoxy. Figure 1 schematically shows the mechanisms of these functionalized MWCNTs.

EXPERIMENTAL

Materials

Multiwalled carbon nanotubes (MWCNTs, C100) were produced by chemical vapor deposition (CVD) process

Correspondence to: C.-C. M. Ma (ccma@che.nthu.edu.tw).

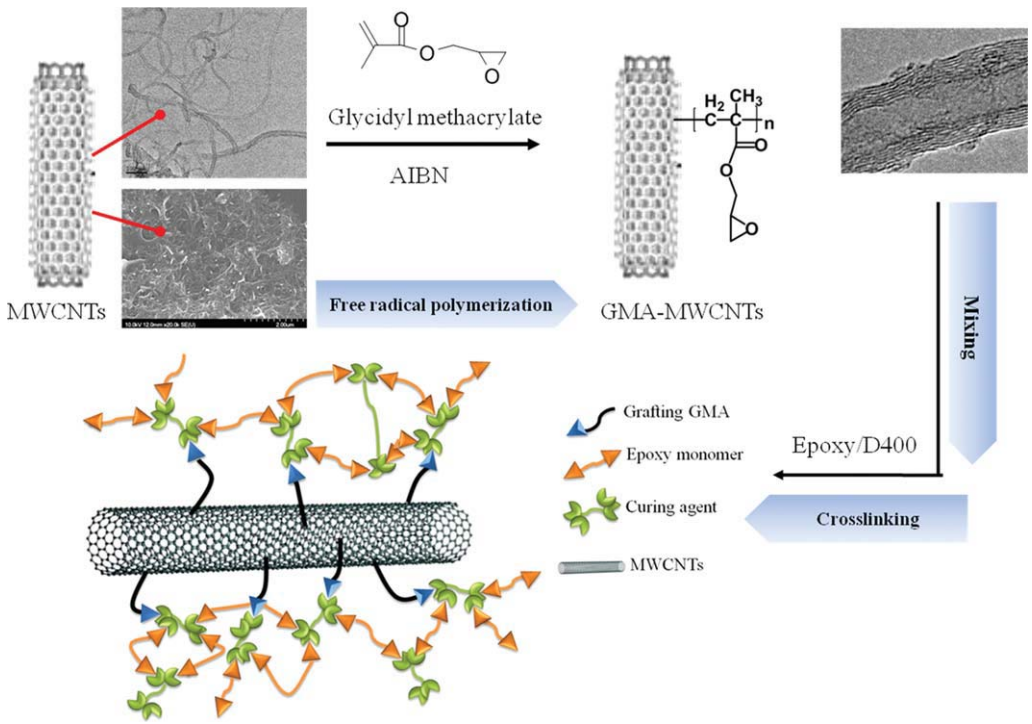

Figure 1 The scheme of functionalization of MWCNTs and the preparation of MWCNTs/epoxy composites. [Color figure can be viewed in the online issue, which is available at wileyonlinelibrary.com.]

and supplied by the CNT Co., Korea. The purity of the MWCNTs was 93%. The diameter of the CNTs was 10–50 nm; the length was 1–25 μm. The diglycidyl ether of bisphenol A (DGEBA) epoxy NPEL-128 was supplied by the Nan Ya Plastics Co. Taiwan, with an epoxide equivalent weight of 190 g/equiv. Jeffamine D400 acted as a curing agent and was supplied by the Huntsman International LLC. The molecular weight is about 400 g/mol. 2,2′-Azobis-isobutyronitrile (AIBN) was obtained from the Showa Chemical Industry Co., Japan. GMA, 1-methyl-2-pyrrolidone (NMP), and acetone were received from the Acros Organic Co., Belgium.

Preparation of GMA-grafted MWCNTs

GMA monomer was de-inhibited using column by celite and sea sand to remove the monomethyl ether hydroquinone (MEHQ) inhibitor. The weight ratio of MWCNTs, NMP, and AIBN was 1 : 290 : 0.4. The MWCNT content was 10 wt % with respect to GMA content. The mixture was sonicated at 65°C under nitrogen atmosphere for 2 h, then stirring for 24 h. After reaction, the GMA-grafted MWCNTs slurry was washed several times with acetone to remove the non-grafted GMA, filtered with 0.2-μm Teflon microfiltration cell and then dried in a vacuum oven for 24 h.

Characterization of GMA-grafted MWCNTs

GMA-grafted MWCNTs were analyzed by thermogravimetric analysis (TGA, TA instrument Q 60) under nitrogen at a heating rate of 10°C/min. Raman spectroscopy were recorded with LabRam I confocal Raman spectrometer. The excitation wavelength was 632.8 nm from He-Ne laser with a laser powder of ~ 15 mW at the sample surface. X-ray photoelectron spectra (XPS) measurements were performed by a PHI Quantera SXM/AES 650 Auger Electron Spectrometer (ULVAC-PHI INC.) equipped with a hemispherical electron analyzer and a scanning monochromated Al Kα ($h\upsilon = 1486.6$ eV) X-ray source. A small spot lens system was allowed to analyze the sample that was less than 1 mm^2 in area. Fourier transform infrared (FTIR) spectroscopy measurements were performed on a Perkin–Elmer RX1 spectrometer and collocated attenuated total reflectance (ATR) equipment. Transmission electron microscopic (TEM) experiments were conducted on a JEM-2100 microscope operated at 200 kV.

Preparation of GMA-grafted MWCNTs/epoxy composite

The functionalized MWCNTs were dispersed in tetrahydrofuran (2 mg/mL) by an ultrasonicator bath for 1 h. Epoxy was added and the solution was stirred for 30 min. The mixture was placed in a warm sonicator bath at 60°C until most of the solvents were removed and then evacuated all solvents. The curing agent was added to the mixture of MWCNTs/epoxy and then stirred for 5 min with a high shear mixer to obtain good homogeneity. The

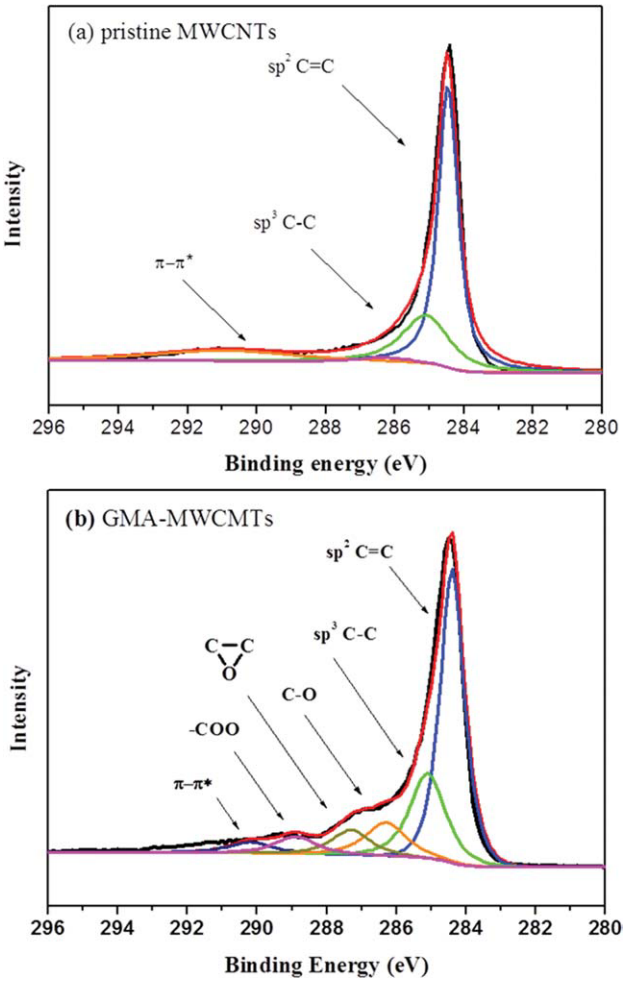

Figure 2 XPS C1s spectra of (a) pristine MWCNTs and (b) functionalized MWCNTs. [Color figure can be viewed in the online issue, which is available at wileyonlinelibrary.com.]

blend was degassed for 1 h in a vacuum oven and then transferred to a mold. The curing condition was 1 h at 60°C, 1 h at 100°C, and 1 h at 160°C. The MWCNTs/epoxy composites were prepared by 1 phr and 3 phr (parts per hundred part of epoxy resin by mass) of MWCNTs.

Characterization of GMA-grafted MWCNTs/epoxy composite

Dynamic mechanical measurements of MWCNTs/epoxy materials (dimension 55 mm × 15 mm × 2 mm) were performed by a TA Instrument DMA Q800 dynamic mechanical analyzer under air at a heating rate of 5°C/min and a frequency of 1 Hz. The thermal conductivity of nanocomposites was measured by a Hot Disk thermal analyzer (TPS2500, Sweden), which is based upon the transient plane source (TPS) method.[14] The dimension of bulk specimens is 50 × 50 × 4 mm with the sensor placed between two similar slabs of materials. The sensor supplied a heat pulse of 0.5 W for 10 s to the sample and associated change in temperature which was recorded. The thermal conductivity of the samples was obtained by fitting the data according to Gustavsson et al.[15]

RESULTS AND DISCUSSION

XPS analysis of GMA-MWCNTs

The XPS analysis was used to investigate the surface compositions of GMA-grafted MWCNTs. Figure 2 presents the results the surface element concentration. The main carbon peak was fitted by several carbon-based functional groups that possess various binding energies.[16] The C1 peaks of pristine MWCNTs can be fitted into two peaks, as indicated in Figure 2(a). The most intense peak at 284.44 eV can be assigned to the C=C bonds of graphene sheets.[17] Meanwhile, the sp^3 carbon atom (C—C bond) appears at 285.1 eV.[17] The binding energy at 290.2 eV can be ascribed to the π–π transition.[17] After grafting GMA on MWCNTs via free radical polymerization, three additional signals appeared in the C1s spectrum [Fig. 2(b)] The peak at 286.30 eV is attributed to the formation of a carbonyl bond (C—O) on the GMA.[16] The important C1s peak at 287.1 eV was the oxirane ring functional group on the GMA chain.[18] In addition, the signal at 288.90 eV was indicated by the —COO bond (ester bond) on the GMA.[16] Unlike pristine MWCNTs, the O1s signal disappeared. This confirmed that GMAs had been grafted on the MWCNTs. Figure 3 shows that the O1s spectra composed of three signals. A peak at 532.31 eV is attributed to the C=O bond of poly(glycidyl methacrylate). The second peak at

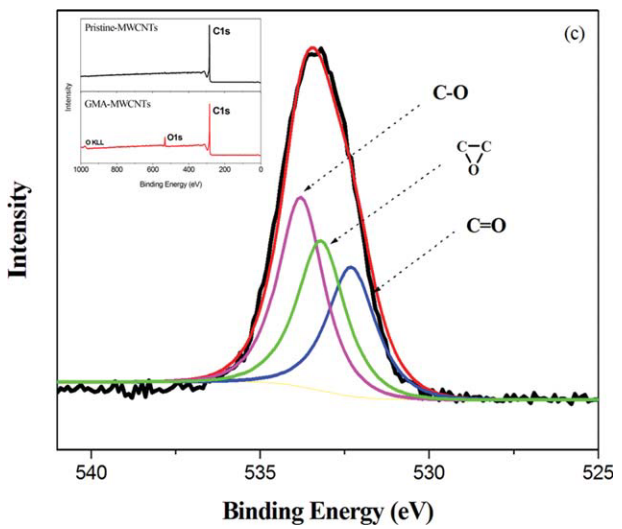

Figure 3 XPS O1s spectra of functionalized MWCNTs. [Color figure can be viewed in the online issue, which is available at wileyonlinelibrary.com.]

533.12 eV is the oxirane ring functional group, and the third peak at 533.79 eV is the C—O bond. The GMA of the oxirane ring group, which is produced by free radical polymerization, the characterization signal was shown in XPS. This indicated that the oxirane ring existed and implied that the open ring reaction does not occur during free radical polymerization. These results further confirmed that GMA was successfully grafted onto the surface of MWCNTs.

In this study, FTIR was also utilized to identify the specific functional groups on the MWCNTs as an evidence of the grafting of GMA. Figure 4 shows that no strong vibrational peaks were observed in the FTIR spectra of pristine MWCNTs. The FTIR spectra of GMA-MWCNTs were compared with those of GMA monomer and GMA-MWCNT mixtures, which the evidence of the grafting of GMA-MWCNTs was presented. The addition peaks of GMA-MWCNTs appeared after free radical polymerization. The vibrational peaks existed at the frequency of 2896 and 1450 cm^{-1} indicating the C—H stretching and C—H bending of GMA polymer chains. The C=O stretching vibrations of ester group existed in GMA-MWCNTs at 1702 cm^{-1}. The peak at 1146 cm^{-1} indicated C(=O)—O stretching of GMA side chains. Furthermore, the C=C stretching of GMA monomer appeared at 1638 cm^{-1}. The AIBN not only initiates GMA but also the MWCNTs by opening π-bonds.[19] The absence of C=C stretching in the FTIR spectra of GMA-MWCNTs indicated that the C=C of the GMA monomer was opened during polymerization, which shows opposite results compared with GMA-MWCNT mixtures. The grafting of polymer chains onto the MWCNTs might be resulted from either direct polymerization of GMA or by the attachment of oligomeric PGMA chains, those specific functional groups shall be appeared.[19] The FTIR spectra of GMA-MWCNT mixtures is similar to that of GMA monomer, implying GMA monomer did not provide covalent bonds with MWCNTs. In addition, three small peaks at 1279, 996, and 868 cm^{-1} appeared in GMA-MWCNTs which were attributed to the vibration of epoxide and those groups originated from the GMA. Furthermore, Figure 4(b) shows different FTIR spectra of GMA-MWCNTs and GMA-MWCNT mixtures after the washing procedure. The FTIR spectra of GMA-MWCNTs presented the identical results after washing procedure. No significant signals were observed in GMA-MWCNT mixtures after washing procedure, indicating the GMA monomer was removed from MWCNTs. Therefore, the FTIR spectra of GMA-MWCNTs imply that GMA was indeed grafted onto MWCNTs by free radical polymerization and the similar results were reported by Wang et al.[20]

The extent of functionalization on MWCNTs can be measured by the percentage of weight retention from the TGA. Figure 5 shows the TGA curves of

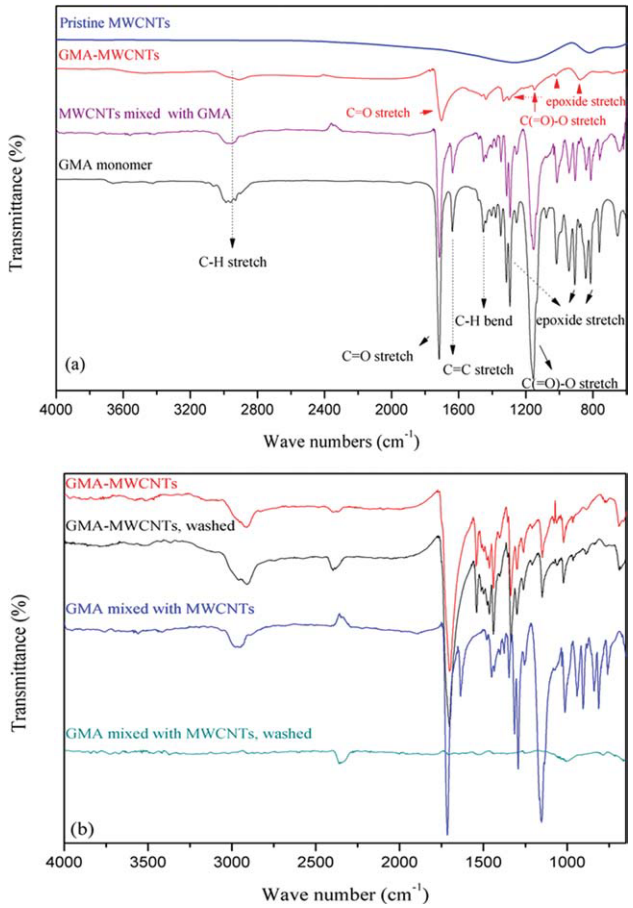

Figure 4 FTIR spectra of pristine MWCNTs, GMA-MWCNTs, pristine MWCNTs containing with GMA, and GMA monomer. [Color figure can be viewed in the online issue, which is available at wileyonlinelibrary.com.]

pristine MWCNTs, GMA-MWCNTs, and GMA monomers. The onset temperature of GMA monomers was at 129°C and the end of decomposition temperature was below 200°C. In contrast to GMA monomer, the TGA curve of GMA-MWCNTs exhibited a significant weight loss about 19 wt % between 150 and 450°C and the onset temperature of thermal degradation was at 253°C. Furthermore, the pristine MWCNTs showed no weight loss up to 450°C. The weight loss of pristine MWCNTs started at 499°C which was attributed to the presence of disordered and amorphous carbons on the surface of pristine MWCNTs.[21] In comparison, the thermal degradation temperature of GMA-MWCNTs is higher than that of GMA monomers, implying the thermal degradation behavior is different. It suggested that the GMA polymer chains were grafted onto the surface of MWCNT. To prove the covalent functionalization between MWCNTs and GMA polymer, the further investigation of GMA-MWCNTs elucidate in the Raman analysis.

Raman spectroscopy was used to analyze the extent of disorder in CNTs. Figure 6 shows the

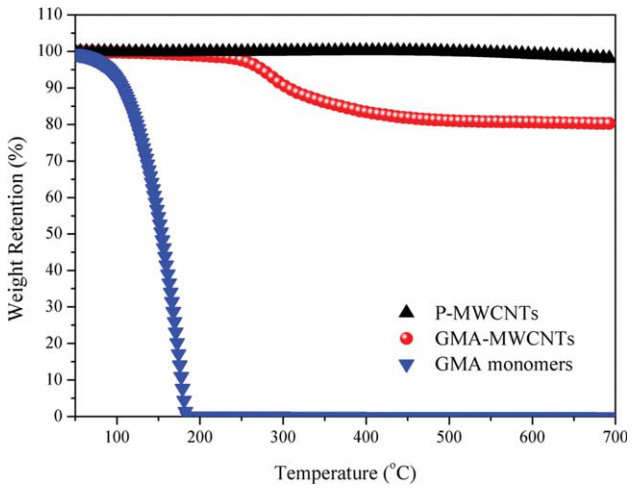

Figure 5 TGA curve of GMA-MWCNTs, GMA monomers, and pristine MWCNTs. [Color figure can be viewed in the online issue, which is available at wileyonlinelibrary.com.]

Raman spectra of the pristine MWCNTs and GMA-MWCNTs. There are two main signals in the range 1200–1700 cm^{-1}, which are the typical Raman peaks of MWCNTs.[22] The range in 1329 cm^{-1} is labeled as the D band. The disorder induced band in the graphite lattice, or defects in the MWCNTs.[23] The G band in the 1580 cm^{-1} corresponded to the Raman active E_{2g} mode, and indicated the crystalline graphite structure in MWCNTs.[24] It is possible to calculate the I_D/I_G ratio to obtain the structural purity of the CNTs. The I_D/I_G value of pristine MWCNTs was 1.04 ± 0.03 and the I_D/I_G value of GMA-MWCNTs increased to 1.35 ± 0.04. This indicates that the MWCNTs were modified by free radical polymerization. The free radical initiators opened the C=C bond in MWCNT during the addition polymerization of GMA. The D′ band at ~ 1610 cm^{-1}, which was also attributed to the defects and disorder in MWCNTs.[25] It was observed that the signal of functionalized MWCNTs is greater than pristine MWCNTs, which is known to be affected by the disorder in nanotubes, implying that GMA was grafted onto MWCNTs. If GMA was attached to the MWCNT surface by a noncovalent interaction, the D band of Raman spectrum will not significantly changed. Consequently, it was concluded that GMA has been successfully grafted onto the MWCNTs according to the combined results of XPS, Raman, and FTIR.[19]

Dispersion ability of GMA-MWCNTs

Figure 7 shows different dispersing abilities of MWCNTs in tetrahydrofuran, including pristine MWCNTs and GMA-MWCNTs. When pristine MWCNTs were stirred with tetrahydrofuran, the pristine MWCNTs aggregated easily and precipitated at the bottom [Fig. 7(a)] Furthermore, after chemical modification of MWCNTs, GMA-MWCNTs possessed an oxirane ring group, which changed the compatibility of pristine MWCNTs with tetrahydrofuran, allowing GMA-MWCNTs to be easily dispersed into low polarity tetrahydrofuran, as shown in Figure 7(b). Moreover, the dispersed solution of GMA-MWCNTs [Fig. 7(c)] did not precipitate after 6 months. In this study, the process of preparing epoxy composites was conducted by tetrahydrofuran for the dispersion of MWCNTs. GMA-MWCNTs is easily dispersed in tetrahydrofuran, also possessing similar functional group with epoxy resin to improve the compatibility with epoxy matrix.

The microstructure of GMA-MWCNTs was investigated by TEM, as shown in Figure 8. The surface of pristine MWCNTs was relatively smooth and clean, due to their high purity. After chemical modification, an extra phase appeared on the sidewall of GMA grafted with GMA-MWCNTs. This specimen was washed by solvent several times. This implied that the individual MWCNTs along with

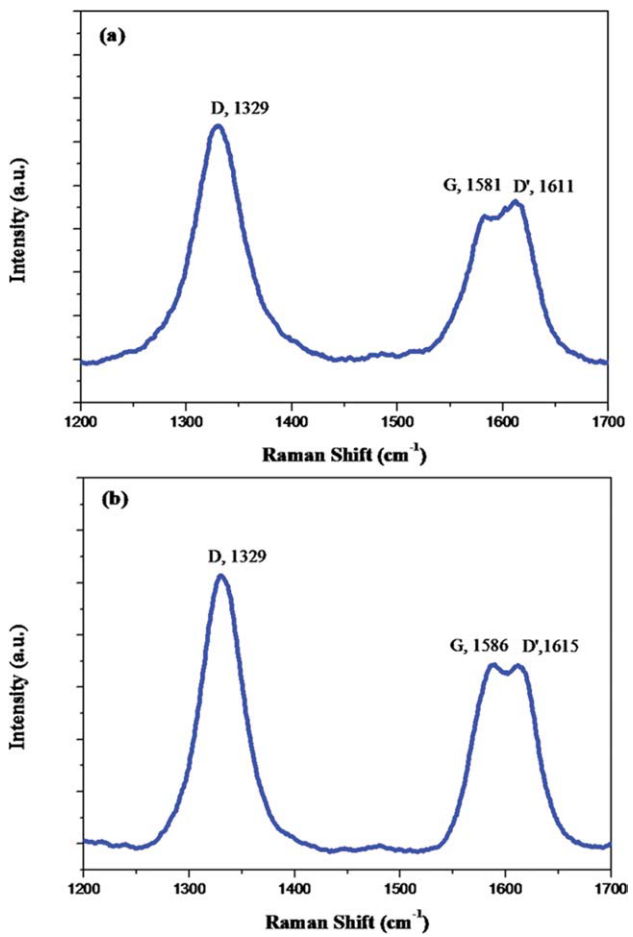

Figure 6 Raman spectra of (a) pristine MWCNTs and (b) GMA-MWCNTs. [Color figure can be viewed in the online issue, which is available at wileyonlinelibrary.com.]

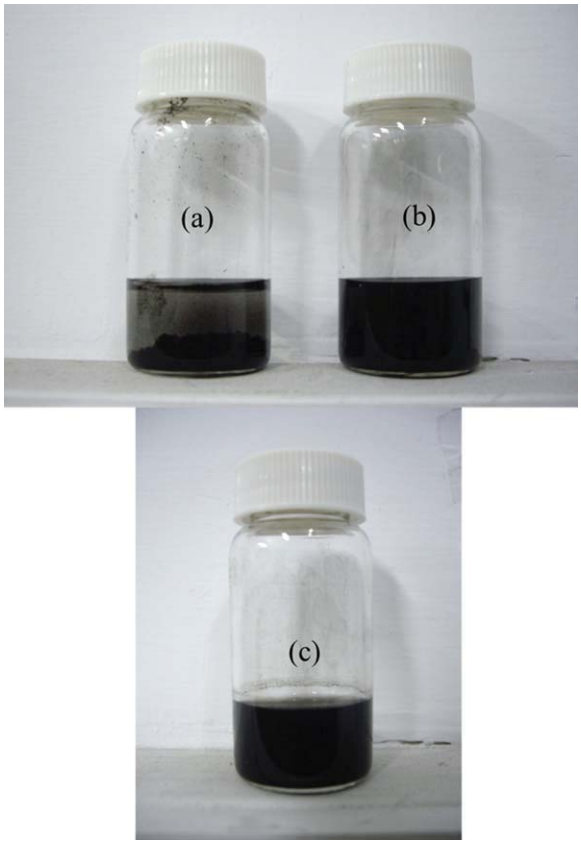

Figure 7 Photograph showing the dispersion of functionalized MWCNTs (a) and pristine MWCNTs (b) in THF. The photographs of (a) and (b) were taken after 1 day of storage at room temperature. The dispersion of functionalized MWCNTs (c) was taken after 6 months of storage at room temperature. [Color figure can be viewed in the online issue, which is available at wileyonlinelibrary.com.]

surrounding amorphous polymer and the grafting reactions have taken place on the MWCNT sidewall, causing that the functionalized MWCNTs can improve the dispersion ability of MWCNTs in organic solvent. The morphology of epoxy nanocomposites was further investigated by TEM (Fig. 9). Pristine MWCNTs was agglomerated in the MWCNTs/epoxy composite were observed. The inhomogeneous dispersion of pristine MWCNTs may be attributed to the strong interaction among the MWCNT itself and the large difference in specific surface energy between MWCNTs and epoxy matrix. GMA-MWCNTs were dispersed well in epoxy matrix, however, there are some small bundles of MWCNTs existed. It also confirmed the dispersion of GMA-MWCNTs in Figure 6.

Dynamical mechanical analysis of MWCNTs/epoxy composites

Figure 10 shows the effect of MWCNT content on the storage modulus (E') of MWCNTs/epoxy composites obtained from dynamic mechanical analysis as a function of temperature (25–100°C). The elastic modulus of epoxy was decreased by three orders of magnitude with increasing temperature, which resulted from the glass-rubber transition.[26] The sudden decrease in the modulus represents the energy dissipation phenomenon involving the motions of the polymer chain. Several studies reported that adding CNTs to polymer matrices caused an increase in the storage modulus.[8,26–28] However, this study shows a decrease of the storage modulus of the pristine MWCNTs/epoxy composites. This result can be attributed to the fact that pristine MWCNTs did not possess good compatibility with epoxy, and therefore cause a decrease in the cross-linking density of epoxy and increase the free volume.[29] Moreover, the curing agent in this study is amine terminated polypropylene glycol, which may easily affect the curing reaction by the steric hindrance of CNTs.

Above the glass transition temperature (T_g), there are no significant differences in the storage modulus

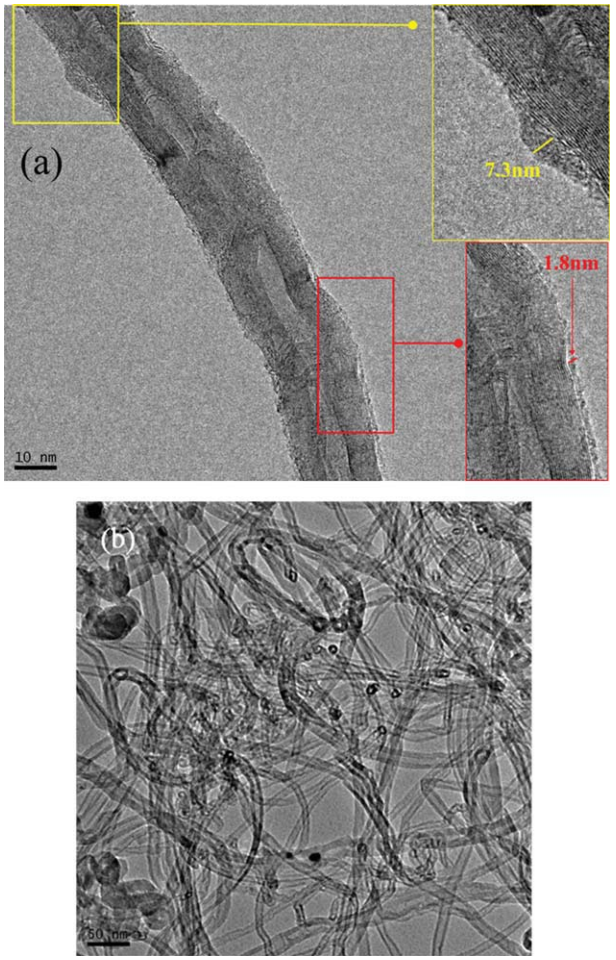

Figure 8 TEM images of functionalized MWCNTs (a) and pristine MWCNTs (b). [Color figure can be viewed in the online issue, which is available at wileyonlinelibrary.com.]

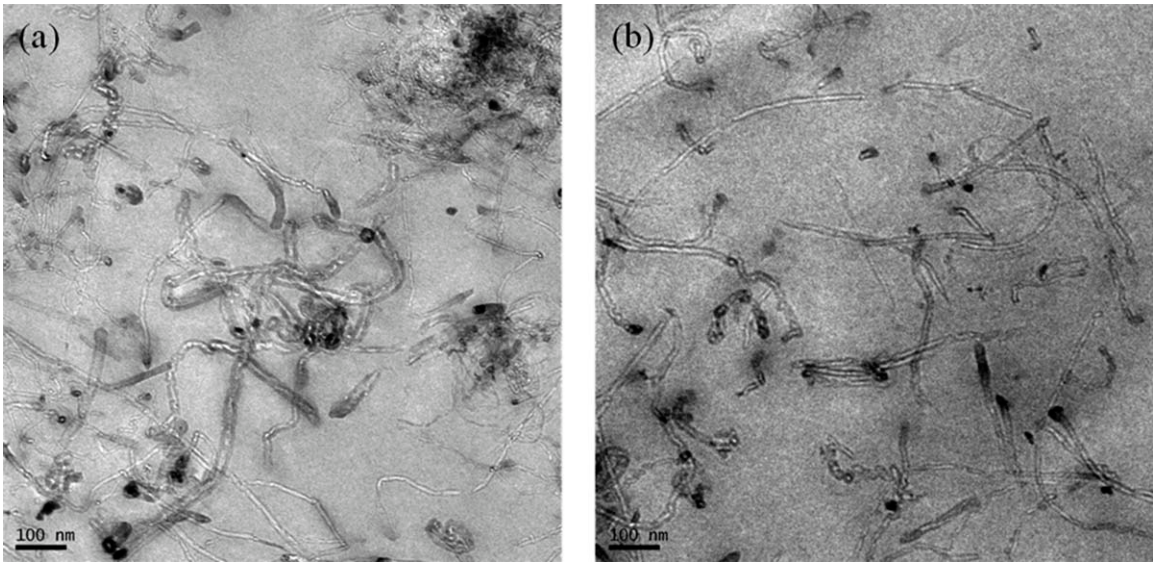

Figure 9 TEM images of epoxy nanocomposites: (a) pristine MWCNTs and (b) GMA-MWCNTs.

when pristine MWCNTs or GMA-MWCNTs were added. Below the T_g, GMA-MWCNTs positively affected the elastic properties of the epoxy matrix. The storage modulus of 3 phr GMA-MWCNTs/epoxy composite at 25°C is 2.91 GPa, and then decreases to 2.87 GPa at 50°C and to 0.04 GPa at 100°C. The storage modulus of neat epoxy at 25°C is 2.48 GPa, 0.32 GPa at 50°C, and 0.01 GPa at 100°C. These results showed that the enhancement of storage modulus for 1 phr GMA-MWCNTs/epoxy at 50°C increased approximately 388% [1.56 GPa compared with neat epoxy (0.32 GPa)] and 3 phr GMA-MWCNTs/epoxy was increased around 518% from the neat epoxy at 50°C [1.98 GPa compared with neat epoxy (0.32 GPa)]. This result was attributed to extremely high modulus of MWCNTs and their interactions with epoxy resin to form dense network structure.[28] Furthermore, the free volume of GMA-MWCNTs/epoxy would be reduced to exhibit a higher dynamic mechanical property.

The peak temperatures of tan δ curves can be defined as T_g.[27] Figures 11 and 12 show that the tan δ and the T_g shifted behavior of epoxy nanocomposites, respectively. The temperature can be obtained corresponding to the decreasing of the area under the tanδ curve when PGMA-MWCNTs content increases, due to functionalized MWCNTs that could enhance the rigidity of epoxy composites, which will reduce the elasticity of epoxy composites. On the other hand, the area of tan δ was increased by adding pristine MWCNTs. Pristine MWCNTs do not possess reactive sites with epoxy resin, which may hinder the curing reaction to reduce the cross-linking density; hence, the composite will possess higher elasticity. The T_g for the nanocomposites obviously increased at high temperatures, and the T_g of the epoxy matrix was 50.5°C, increasing to 56.8°C for 3 phr pristine MWCNTs/epoxy composites and increasing to 61.7°C for 3 phr GMA-MWCNTs/epoxy composites. After adding different contents of pristine MWCNTs to the epoxy, the T_g of 3 phr pristine MWCNTs/epoxy were similar to 1 phr pristine MWCNTs/epoxy, because the unmodified MWCNTs are easily agglomerated to reduce the reinforcement effect. Therefore, the increase of T_g and the storage modulus for epoxy matrix by GMA-MWCNTs could be interpreted as the decrease of chain mobility. The steric hindrance of MWCNTs and the functional group was based on MWCNTs,

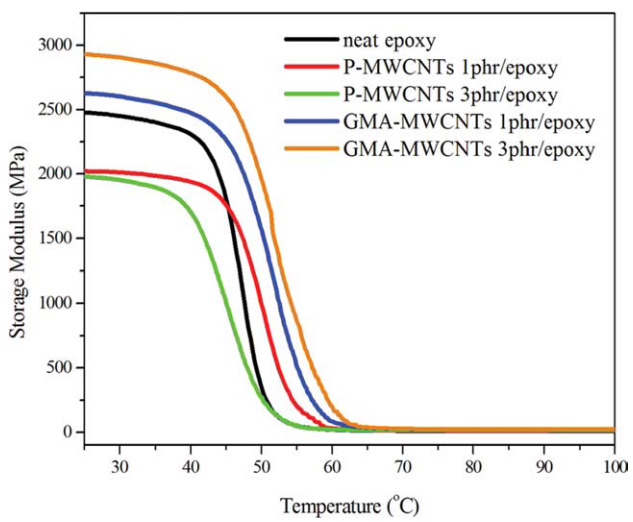

Figure 10 Storage modulus of epoxy nanocomposites with pristine MWCNTs ratio of 1 phr and 3 phr; and GMA-MWCNTs ratio of 1 phr and 3 phr. [Color figure can be viewed in the online issue, which is available at wileyonlinelibrary.com.]

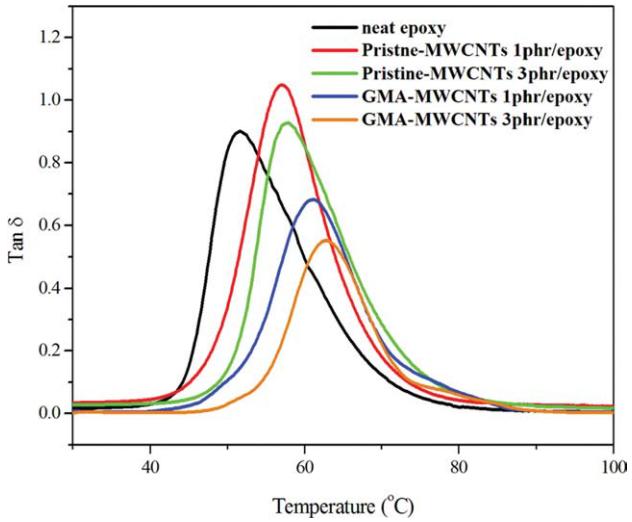

Figure 11 Tan δ of epoxy and nanocomposites with pristine MWCNTs ratio of 1 phr and 3 phr; and GMA-MWCNTs ratio of 1 phr and 3 phr. [Color figure can be viewed in the online issue, which is available at wileyonlinelibrary.com.]

which could react with the epoxy, increase the cross-linking extent to form rigid networks.

Thermal conductivity of MWCNTs/epoxy composites

The high aspect ratio and the huge surface area of CNTs strongly affect the thermal conductivity of nanocomposites. High aspect ratio and highly thermal conductivity of fillers provide a conduction of phonons over a long distance without any transitions from particle to particle. Although, the thermal conductivity of general filler is 100 times higher than that of the polymer matrix, there is no significant enhancement in the thermal conductivity of the composites by the experimental results.[30] Theoretically, the transport of thermal energy in CNTs could be related to a phonon conduction mechanism, including the number of phonon active modes, the boundary surface scattering, the length of the free path for electrons and phonons, and Umklapp scattering.[31]

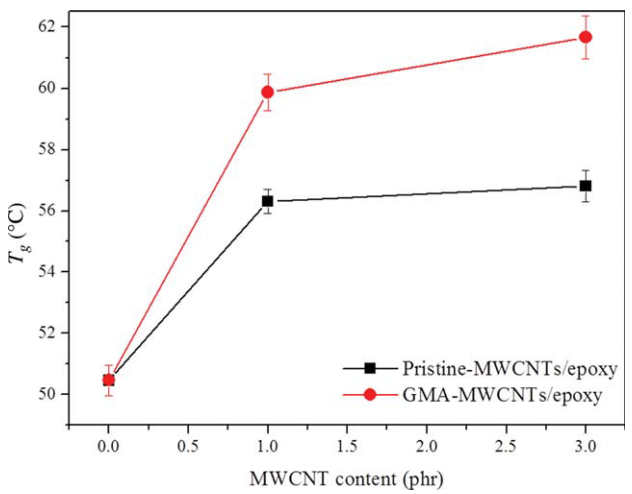

Figure 12 Glass transition temperature (T_g) of MWCNTs/epoxy composites with different pristine MWCNTs and GMA-MWCNTs contents. [Color figure can be viewed in the online issue, which is available at wileyonlinelibrary.com.]

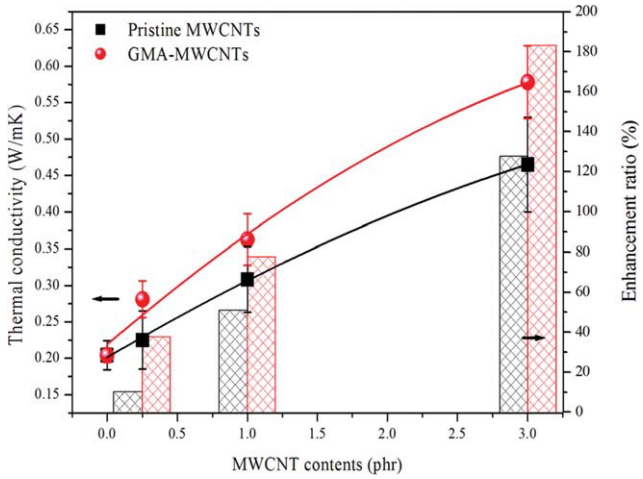

Figure 13 Thermal conductivity of nanocomposites with various contents of pristine MWCNTs and GMA MWCNTs. [Color figure can be viewed in the online issue, which is available at wileyonlinelibrary.com.]

The thermal conductivity of GMA-MWCNTs/epoxy composites exhibits a significant increase compared with pristine MWCNTs/epoxy composites. Thermal conductivity of GMA-MWCNTs/epoxy composites increased around 78% (0.3626 W/mK) by adding 1 phr GMA-MWCNTs, and increased 183% (0.5781 W/mK) by adding 3 phr GMA-MWCNTs, as shown in Figure 13. The significant enhancement of thermal conductivity could be explained by the good interfacial adhesion between CNTs and epoxy to affect the phonon conduction. Good dispersion of GMA-MWCNTs in the epoxy matrix will increase the heat flow channel. When polymer matrix contains high MWCNTs content, MWCNTs form bundle structure to cause the reciprocal phonon vector phenomenon.[32] Hence, the thermal conductivity of pristine MWCNTs/epoxy composite exhibits a slight increase (51%, 0.3082 W/mK) by adding 1 phr pristine MWCNTs, increasing 128% (0.4650 W/mK) by adding 3 phr pristine MWCNTs. Due to the agglomeration of pristine MWCNTs will form micro structure to reduce the aspect ratio and form inhomogeneous structure in matrix. In other words, the bundle of MWCNTs will lead to the phonon–phonon umklapp scattering on tube–tube interconnections, consequently reducing

the thermal transport capability,[33,34] dominating the relative enhancement of the thermal conductivity.

CONCLUSIONS

The surface functionalized MWCNTs were successful grafting of GMA onto MWCNTs by free radical polymerization, which appeared to be effective in enhancing dispersion in epoxy matrix. The incorporation of GMA-MWCNTs exhibited better reinforcing effect on the thermal properties compared with pristine MWCNTs. This indicated that the GMA-MWCNTs can react with epoxy through covalent integration to enhance the interfacial interaction, which can reduce the thermal interfacial resistance between GMA-MWCNTs and epoxy matrix. Furthermore, the good compatibility could provide more complete network structure due to the extended area of MWCNTs-epoxy contact. Consequently, the thermal conductivity and T_g of epoxy composite containing with 3 phr GMA-MWCNTs were increased 183% and 11°C, respectively. This suggested that the effective modification of MWCNTs was important for the potential of MWCNTs in enhancing thermal properties of epoxy composites.

References

1. Wu, H. X.; Tong, R.; Qiu, X. Q.; Yang, H. F.; Lin, Y. H.; Cai, R. F.; Qian, S. X. Carbon 2007, 45, 152.
2. Hirsch, A.; Vostrowsky, O. Top Curr Chem 2005, 245, 193.
3. Yu, J.; Grossiord, N.; Koning, C. E.; Loos, J. Carbon 2007, 45, 618.
4. Sung, J. H.; Kim, H. S.; Jin, H. J.; Choi, H. J.; Chin, I. J. Macromolecules 2004, 37, 9899.
5. Yuen, S. M.; Ma, C. C. M.; Chiang, C. L.; Lin, Y. Y.; Teng, C. C. J Polym Sci Part A: Polym Chem 2007, 45, 3349.
6. Shaffer, M. S. P.; Koziol, K. Chem Commun 2002, 18, 2074.
7. Park, S. J.; Cho, M. S.; Lim, S. T.; Choi, H. J.; Jhon, M. S. Macromol Rapid Commun 2003, 24, 1070.
8. Hwang, G. H.; Shieh, Y. T.; Hwang, K. C. Adv Funct Mater 2004, 14, 487.
9. Clayton, L. M.; Sikder, A. K.; Kumar, A.; Cinke, M.; Meyyappan, M.; Gerasimov, T. G.; Harmon, J. P. Adv Funct Mater 2005, 15, 101.
10. Wu, H. X.; Qiu, X. Q.; Cai, R. F.; Qian, S. X. Appl Surf Sci 2007, 253, 5122.
11. Sobkowicz, M. J.; Dorgan, J. R.; Gneshin, K. W.; Herring, A. M.; McKinnon, J. T. J Aust Chem 2009, 62, 865.
12. Shen, J.; Huang, W.; Wu, L.; Hu, Y.; Ye, M. Compos Sci Technol 2007, 67, 3041.
13. Lau, K. T.; Lu, M.; Liao, K. Compos Part A—Appl S 2006, 37, 1837.
14. Zhu, D.; Li, X.; Wang, N.; Wang, X.; Gao, J.; Li, H. Curr Appl Phys 2009, 9, 131.
15. Gustavsson, M.; Karawacki, E.; Gustafsson, S. E. Rev Sci Instrum 1994, 65, 3856.
16. Liu, L.; Qin, Y.; Guo, Z. X.; Zhu, D. Carbon 2003, 41, 331.
17. Zhang, G.; Sun, S.; Yang, D.; Dodelet, J. P.; Sacher, E. Carbon 2008, 46, 196.
18. Beamson, G.; Briggs, D. High Resolution XPS of Organic Polymers: The Scienta ESCA300 Database, Wiley: New York, NY, 1992.
19. Park, S. J.; Cho, M. S.; Lim, S. T.; Choi, H. J.; Jhon, M. S. Marcomol Rapid Commun 2005, 26, 1563.
20. Wang, S.; Liang, R.; Wang, B.; Zhang, C. Carbon 2007, 45, 3042.
21. Yang, S. Y.; Ma, C. C. M.; Teng, C. C.; Huang, Y. W.; Liao, S. H.; Huang, Y. L.; Tien, H. W.; Lee, T. M.; Chiou, K. C. Carbon 2010, 48, 592.
22. Li, Q.; Ni, Z.; Gong, J.; Zhu, D.; Zhu, Z. Carbon 2008, 46, 434.
23. Rai, P.; Mohapatra, D. R.; Hazra, K. S.; Misra, D. S.; Ghatak, J. Chem Phys Lett 2008, 455, 83.
24. Kasuya, A.; Saito, Y.; Sasaki, Y.; Fukushima, M.; Maeda, T.; Horie, C.; Nishina, Y. Mater Sci Eng A: Struct 1996, 218, 46.
25. Zhang, Y.; He, H.; Gao, C. Macromolecules 2008, 41, 9581.
26. Bhattacharyya, S.; Sinturel, C.; Bahloul, O.; Saboungi, M. L.; Thomas, S.; Salvetat, J. P. Carbon 2008, 46, 1037.
27. Chen, Q.; Xu, R.; Yu, D. Polymer 2006, 47, 7711.
28. Xiong, J.; Zheng, Z.; Qin, X.; Li, M.; Li, H.; Wang, X. Carbon 2006, 44, 2701.
29. Gunes, I. S.; Pérez-Bolivar, C.; Cao, F.; Jimenez, G. A.; Anzenbacher, P.; Jana, S. C. J Mater Chem 2010, 20, 3467.
30. Lee, G. W.; Park, M.; Kim, J.; Lee, J. I.; Yoon, H. G. Compos Part A—Appl S 2006, 37, 727.
31. Gojny, F. H.; Wichmann, M. H. G.; Fiedler, B.; Kinloch, I. A.; Bauhofer, W.; Windle, A. H.; Schulte, K. Polymer 2006, 47, 2036.
32. Kim, P.; Shi, L.; Majumdar, A.; McEuen, P. L. Phys Rev Lett 2001, 87, 215502.
33. Aliev, A. E.; Guthy, C.; Zhang, M.; Fang, S.; Zakhidov, A. A.; Fischer, J. E.; Baughman, R. H. Carbon 2007, 45, 2880.
34. Xie, H.; Cai, A.; Wang, X. Phys Lett A 2007, 369, 120.